MAJOR ARTICLE

Neuronal Bioenergetics and Acute Mitochondrial Dysfunction: A Clue to Understanding the Central Nervous System Side Effects of Efavirenz

Haryes A. Funes,[1,3,a] Nadezda Apostolova,[4,5,a] Fernando Alegre,[1,3] Ana Blas-Garcia,[1,3] Angeles Alvarez,[1,2,4] Miguel Marti-Cabrera,[1,4] and Juan V. Esplugues[1,3,4]

[1]Departamento de Farmacología, Facultad de Medicina, and [2]Fundación General, Universidad de Valencia, [3]FISABIO–Hospital Universitario Dr. Peset, and [4]CIBERehd, Valencia, and [5]Facultad de Ciencias de la Salud, Universidad Jaime I, Castellón de la Plana, Spain

Background. Neurological pathogenesis is associated with mitochondrial dysfunction and differences in neuronal/glial handling of oxygen and glucose. The main side effects attributed to efavirenz involve the CNS, but the underlying mechanisms are unclear.

Methods. Human cell lines and rat primary cultures of neurons and astrocytes were treated with clinically relevant efavirenz concentration.

Results. Efavirenz alters mitochondrial respiration, enhances reactive oxygen species generation, undermines mitochondrial membrane potential, and reduces adenosine triphosphate (ATP) levels in a concentration-dependent fashion in both neurons and glia. However, it triggers adenosine monophosphate–activated protein kinase only in glia, upregulating glycolysis and increasing intracellular ATP levels, which do not occur in neurons. To reproduce the conditions that often exist in human immunodeficiency virus–related neuroinflammatory disorders, the effects of efavirenz were evaluated in the presence of exogenous nitric oxide, an inflammatory mediator and mitochondrial inhibitor. The combination potentiated the effects on mitochondrial parameters in both neurons and glia, but ATP generation and lactate production were enhanced only in glia.

Conclusions. Efavirenz affects the bioenergetics of neurons through a mechanism involving acute mitochondrial inhibition, an action exacerbated in neuroinflammatory conditions. A similar scenario of glia survival and degeneration of neurons with signs of mitochondrial dysfunction and oxidative stress has been associated with neurocognitive disorders.

Keywords. Mitochondria; neurotoxicity; HIV; nitric oxide; central nervous system; efavirenz; HIV-associated neurocognitive disorders.

There is growing evidence that neurological pathogenesis is often linked to mitochondrial dysfunction and the way neurons and glia handle oxygen/glucose. It has been shown that astrocytes are protected from mitochondrial inhibition by the rapid upregulation of adenosine monophosphate (AMP)–activated protein kinase (AMPK)–mediated glycolysis. Neurons, on the other hand, lack this defense mechanism and are therefore more vulnerable [1, 2]. This action is relevant given that several neurodegenerative diseases, including human immunodeficiency virus (HIV)–associated neurocognitive disorders, are characterized by the selective damage of neurons versus glial cell survival [3]. In this context, the aforementioned action could also underlie drug-induced brain toxicity.

The nonnucleoside reverse transcriptase inhibitor (NNRTI) efavirenz (EFV) is a widely prescribed anti-HIV drug. However, many patients exhibit central nervous system (CNS)–related side effects, including dizziness, a hangover-like sensation, impaired concentration,

Received 18 December 2013; accepted 28 April 2014.

[a]H. A. F. and N. A. contributed equally to this report.

Presented in part: 15th International Workshop on Comorbidities and Adverse Drug Reactions in HIV, Brussels, Belgium, 15–17 October 2013; 2014 Conference on Retroviruses and Opportunistic Infections, Boston, Massachusetts, 3–7 March 2014; several meetings throughout Spain about HIV/AIDS.

Correspondence: Nadezda Apostolova, PhD, Av. Vicent Sos Baynat s/n, 12071 Castellón de la Plana, Spain (nadezda.apostolova@uv.es).

The Journal of Infectious Diseases

DOI: 10.1093/infdis/jiu273

nervousness, sleep disturbances, psychosis, suicidal ideation, and neurocognitive impairment. In some cases, these effects are so severe that the therapy requires discontinuation [4–6]. The mechanism of toxicity in the CNS is yet to be determined, although certain evidence implicates mitochondria. For example, EFV has been shown to affect mitochondrial oxidative phosphorylation in the mouse brain [7]. In hepatic cells, this drug undermined mitochondrial function, leading to the activation of AMPK, the master switch of cellular bioenergetics. Such a response was compound specific, as it was not reproduced by nevirapine, another widely prescribed NNRTI, and was unrelated to the interference of mitochondrial DNA replication commonly associated with other anti-HIV drugs [8, 9].

In light of this evidence, we analyzed the actions of EFV in neurons and glia the possible interference with mitochondria, and the effect on glycolysis. In addition, since HIV infection is often accompanied by neuroinflammation [10], we evaluated the way nitric oxide (NO), a well-known mediator of inflammation and inhibitor of mitochondrial function, affects the aforementioned actions of EFV.

MATERIALS AND METHODS

Reagents and Treatments

Unless otherwise stated, chemicals were from Sigma-Aldrich (Steinheim, Germany). EFV (Sequoia Research Products, Pangbourne, United Kingdom) was dissolved in methanol (3 mg/mL). Methanol 0.25%, which did not have a significant impact on any of the parameters studied, was used for all EFV treatments and vehicle control experiments, and statistical analyses of differences between findings of these tests was performed. In the experiments with exogenous NO, cells were treated with 0.3-mM (for neurons) or 0.5-mM (for glia) concentrations of DETA-NO ((Z)-1-[2-aminoethyl)-N-(2-ammonioethyl)amino]diazen-1-ium-1,2-diolate; Alexis, San Diego, CA), which are capable of inhibiting cellular respiration [11]. Immediate NO exposure was ensured by preheating (at 37°C for 20 minutes) the freshly prepared DETA-NO/Milli-Q water solution before application. For the co-treatments, DETA-NO was added 1 hour before EFV administration.

Cell Culture

Unless stated otherwise, reagents were from Gibco (Invitrogen, Eugene, OR). Cell cultures were maintained in an incubator (IGO 150, Jouan, Saint-Herblain Cedes, France) at 37°C in a humidified atmosphere of 5% CO_2 and 95% air (AirLiquide Medicinal, Valencia, Spain). Experiments were performed with subconfluent cultures in complete medium supplemented with 3% (v/v) heat-inactivated fetal bovine serum (FBS). The human glioma cell line U-251MG (CLS 300385) was cultured in Dulbecco's modified Eagle's medium (DMEM; Sigma-Aldrich), and the human neuroblastoma cell line SH-SY5Y (ATCC CRL-2266) was cultured in Roswell Park Memorial Institute 1640 medium supplemented with 2.383 g/L HEPES, 1.5 g/L sodium bicarbonate, and 110 mg/L sodium pyruvate. Both media contained 4.5 g/L glucose and were supplemented with 10% FBS, 1 mM NEAA, 2 mM L-glutamine, penicillin (50 units/mL), and streptomycin (50 µg/mL). SH-SY5Y cells were differentiated into neurons prior to treatment. A 1-mM concentration of db-cAMP (N(6),2′-O-dibutyryladenosine 3′:5′ cyclic monophosphate) [12] was added 1 day after seeding, and cells were then allowed to differentiate for 6 days, with medium replaced every 48 hours.

Primary cultures of astrocytes and neurons were obtained from rat cerebral cortex [13]. In brief, astrocytes from neonatal (24-hours-old) Wistar rats were seeded (1.2×10^5 cells/cm^2 in 150-cm^2 flasks) in DMEM supplemented with 10% FBS and cultured for 12–14 days. Under these conditions, astrocytes represented 85% of the cells, the remaining proportion being microglia and progenitor cells. Primary cultures of neurons were prepared from rat fetuses at gestation day 15, cell suspensions were plated (2.5×10^5 cells/cm^2 in plates or flasks previously coated with 15 µg/mL poly-D-lysine) in DMEM supplemented with 10% FBS; 48 hours later the medium was replaced with DMEM supplemented with 5% horse serum, 20 mM D-glucose, and 10 µM cytosine arabinoside (to prevent nonneuronal proliferation). Neurons were used on day 7, when the presence of neurofilaments was evident in 99% of the cells. The protocols regarding isolation and primary cell culture complied with European Community guidelines for the use of animal experimental models and were approved by the Ethics Committee of the University of Valencia.

Cell Viability

Cell viability was studied by the colorimetric MTT [3-(4,5-dimethylthiazol-2-yl)-2,5-diprenyl tetrazolium bromide] assay. U-251MG cells (2×10^4 cells/cm^2), SH-SY5Y (1.5×10^4 cells/cm^2), primary neurons (2.5×10^5 cells/cm^2), and astrocytes (2×10^4 cells/cm^2) were allowed to attach in 96-well plates. MTT reagent (Roche Diagnostics, Mannheim, Germany) was added (20 µL/well) during the last 4 hours of the 24-hour treatment period; cells were then dissolved in DMSO (100 µL/well) for 5 minutes at 37°C, and absorbance was measured by a Multiskan plate-reader spectrophotometer (Thermo Labsystems, Thermo Scientific, Rockford, IL).

Fluorescence Microscopy and Static Cytometry

The signal was detected (Olympus IX81 microscope) and quantified using ScanR static cytometry software, version 2.03.2 (Olympus, Hamburg, Germany). U-251MG (3×10^4 cells/cm^2), SH-SY5Y (1.5×10^4 cells/cm^2), primary neurons (2.5×10^5/cm^2), and astrocytes (4×10^4 cells/cm^2) were treated in duplicate in 48-well plates and washed in Hank's balanced salt solution (HBSS), and 16–20 life-cell images/well were immediately recorded.

Cell Proliferation and Survival

Cells proliferated exponentially for 24 hours in the presence of vehicle, EFV, DETA-NO, or EFV + DETA-NO and then were counted according to Hoechst fluorescence (1 μM Hoechst 33 342; 25 images/well).

Mitochondrial Superoxide Production and Mitochondrial Membrane Potential ($\Delta\psi_m$)

Cells were treated for 6 hours and/or 24 hours in vehicle, EFV, DETA-NO, or EFV + DETA-NO, and fluorochromes, 1 μM Hoechst 33 342, and either 2.5 μM MitoSOX (for superoxide analysis) or 2.5 μM TMRM (for $\Delta\psi_m$ analysis; Molecular Probes, Invitrogen, Eugene, OR) were added for the last 30 minutes of treatment. Rotenone 10 μM (a widely used inhibitor of mitochondrial complex I) and FCCP 10 μM (a pharmacological uncoupler of mitochondrial oxidative phosphorylation) were used as positive controls for analyses of superoxide production and $\Delta\psi_m$, respectively.

Metabolite Determinations

The level of intracellular adenosine triphosphate (ATP) was determined in cells incubated for 24 hours (with EFV, DETA-NO, or DETA-NO + EFV) by the ATP Bioluminescence Assay Kit HSII (Roche Diagnostics) and a Fluoroskan microplate reader (Thermo Labsystems). The lactate concentration in the extracellular medium was evaluated in 96-well plates, using the Lactate Assay Kit (BioVision, San Francisco, CA) and a Multiskan plate reader spectrophotometer (Thermo Labsystems). For both metabolites, protein concentrations were determined using the BCA protein assay kit (Pierce Chemicals, Boulder, CO).

Electrochemical Measurement of Oxygen (O_2) Consumption

Cells (5×10^6 per 1 mL of HBSS) were agitated in a gas-tight chamber at 37°C. Measurements were taken with a Clark-type O_2 electrode (Rank Brothers, Bottisham, United Kingdom) and recorded with the Duo.18 data acquisition device (WPI, Stevenage, United Kingdom) immediately after addition of EFV (10, 25 μM), DETA-NO, or the respective solvents.

Protein Extract Isolation and Western Blotting

Total protein extracts of cells treated for 6 hours were isolated, and immunoblotting was performed as described previously [8]. In brief, cell pellets were lysed in PhosphoSafe lysis buffer (Novagen, Calbiochem, La Jolla, CA) supplemented with protease inhibitors (Complete Mini protease inhibitor cocktail, Roche Diagnostics) to ensure preservation of the phosphorylated form of AMPK. In some experiments, the AMPK inhibitor compound C (6-[4-(2-Piperidin-1-ylethoxy)-phenyl)]-3-pyridin-4-ylpyrazolo[1,5-a]pyrimidine, Calbiochem, La Jolla, CA) was added 30 minutes before EFV administration and throughout the 6- or 24-hour incubation period. Samples were vortexed, incubated for 5 minutes, vortexed a second time, and centrifuged at 16 100 ×*g* for 5 minutes at 4°C. The total protein concentration was quantified by the BCA protein assay kit (Pierce Chemicals), and equal amounts of protein (40 μg) were loaded onto sodium dodecyl sulfate polyacrylamide gels and analyzed by Western blotting (BioRad, Hercules, CA), using anti-AMPK alpha 1 + alpha 2 (phospho T172) polyclonal antibody (1:1000, Abcam, Cambridge, United Kingdom) or anti-actin (1:1000 [primary antibody]; Sigma-Aldrich, primary antibody) and peroxidase-labeled anti-rabbit IgG (1:5000 [secondary antibody]; Vector laboratories, Burlingame, CA). Protein bands were detected by a LAS-3000 digital luminescent image analyzer (Fujifilm), using the enhanced chemiluminescent reagent ECL (Amersham, GE Healthcare, Little Chalfont, United Kingdom) or SuperSignal WestFemto (Pierce Chemicals). Protein expression was quantified by means of densitometry (Image Gauge software, version 4.0, Fujifilm). Data were normalized to values for actin, and results are expressed as the percentage induction relative to the control group.

Presentation of Data and Statistical Analysis

Data were analyzed by means of the Student *t* test (GraphPad Prism software, version 5). All values are mean ± standard error of the mean, and statistical significance was defined as a *P* value of <.05. In most cases, data are represented as the percentage of the value for the negative control, with the negative control (untreated cells) considered 100%.

RESULTS

EFV Disrupts Mitochondrial Function and Compromises Cell Viability

Acute EFV treatment (10 μM and 25 μM) diminished O_2 consumption rapidly and in a concentration-dependent manner in SH-SY5Y (neurons) and U-251MG (glia; Figure 1*A*). In addition, 2 parameters of mitochondrial function were affected in both cell populations (6 and 24 hours). First, fluorescence microscopy revealed a significant and concentration/time-dependent increase in superoxide production (Figure 1*B*). Second, EFV produced a major reduction in $\Delta\psi_m$ that was slightly more pronounced in glia than in neurons (Figure 1*C*). Additionally, cell viability/proliferation in SH-SY5Y was reduced in a concentration-dependent manner following 24 hours of incubation, an effect not observed in U-251MG (Figure 1*D*). The results obtained in neuroblastoma and glioma cell lines were reproduced in primary cultures of rat neurons and astrocytes (Figure 2). Thus, an increase in mitochondrial superoxide generation and a decrease in $\Delta\psi_m$ (Figure 2*A* and 2*B*, respectively) were observed in both cell populations after 24 hours of treatment. Moreover, the viability of neurons was substantially compromised by EFV, while that of astrocytes was only slightly affected by the higher concentration of EFV (Figure 2*C*). These data show that the deleterious action of EFV on mitochondrial function previously reported in hepatocytes is also

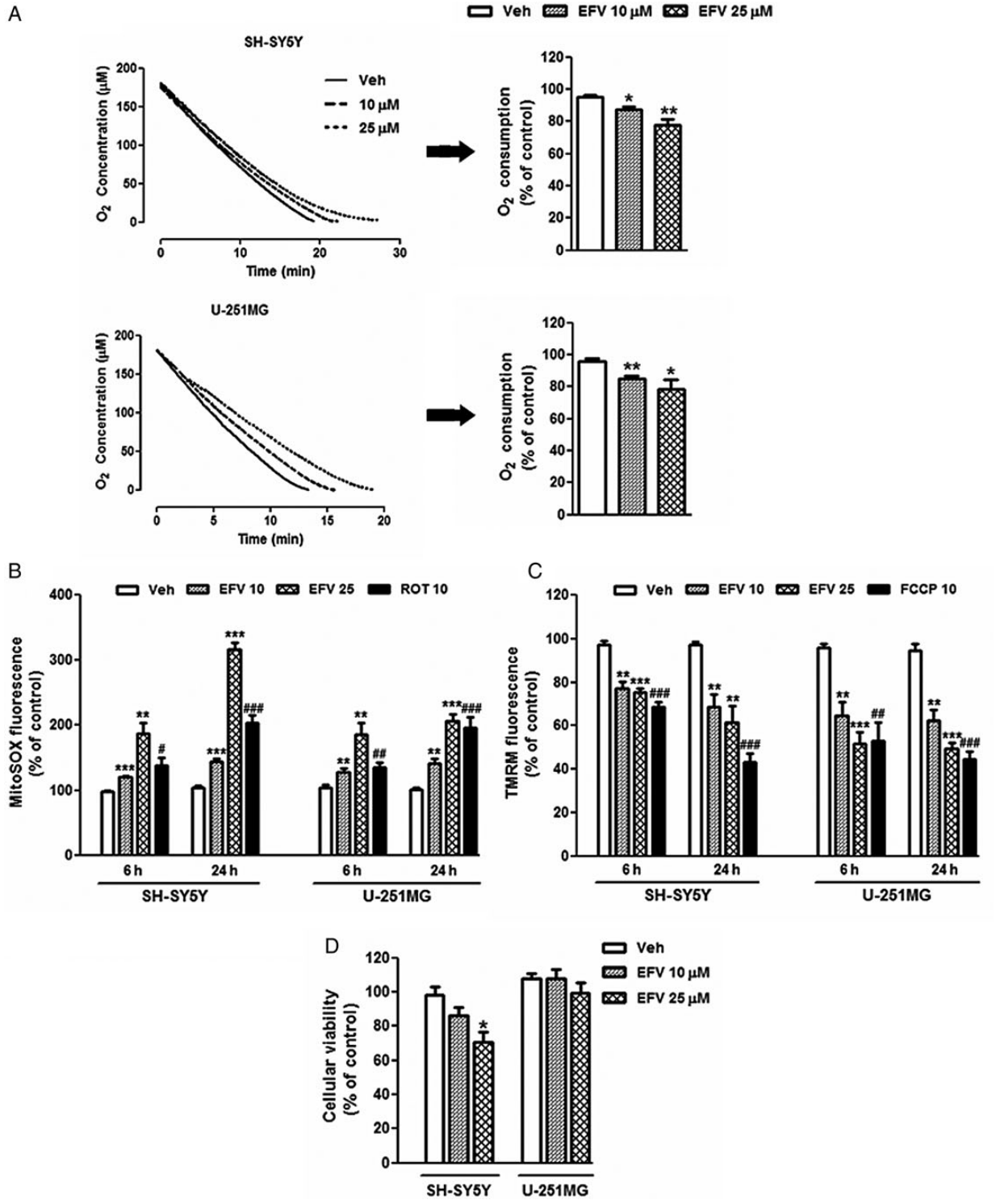

Figure 1. Effect of efavirenz (EFV) on mitochondrial function in SH-SY5Y (neuroblastoma cells) and U-251MG (glioma cells). *A*, Efavirenz acutely decreases O_2 consumption. Representative traces and quantification of data showing the rate of O_2 consumption (Clark-type O_2 electrode) in the absence (vehicle; Veh) and presence of EFV 10 µM and 25 µM. *B* and *C*, Determination of superoxide production, expressed as relative MitoSOX fluorescence (*B*), and mitochondrial membrane potential, expressed as relative TMRM fluorescence (*C*), in cells treated with increasing concentrations of EFV or vehicle for 6 and 24 hours, using rotenone (ROT) and FCCP (both at 10 µM) as positive controls, respectively. *D*, Effect of EFV (24 hours) on cell viability according to the MTT assay; results represent relative absorbance ($\lambda = 570$ nm) and are expressed as the percentage of the absorbance recorded in untreated cells. Data (mean ± standard error of the mean; n = 3–5) were compared with those of untreated cells (the values for which were considered 100%) and analyzed by the Student *t* test. $^{*}P < .05$, $^{**}P < .01$, and $^{***}P < .001$, compared with vehicle; $^{\#}P < .05$, $^{\#\#}P < .01$, and $^{\#\#\#}P < .001$, for comparisons of ROT and FCCP values to those for untreated cells.

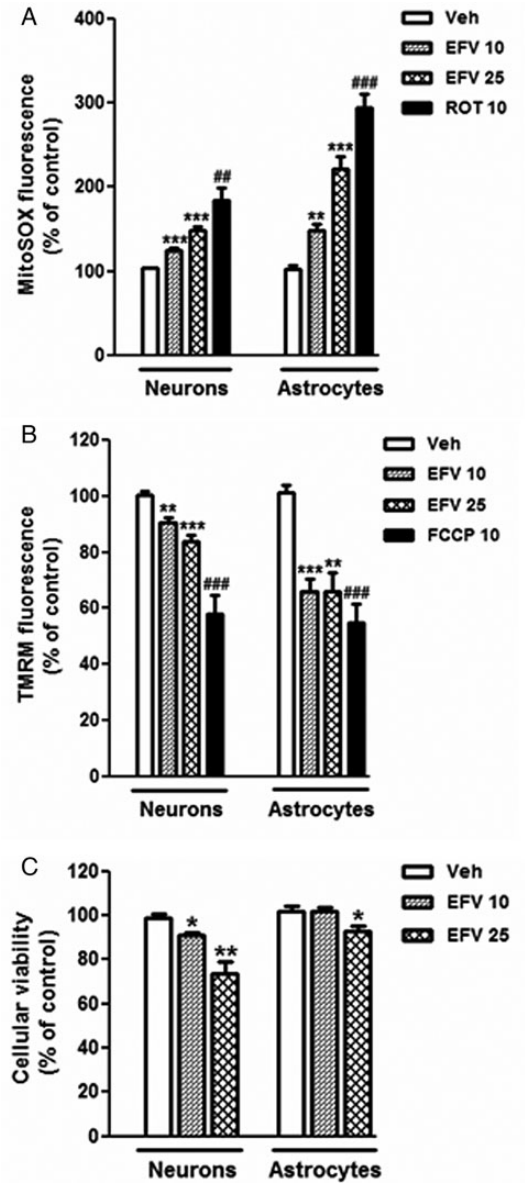

Figure 2. Effect of efavirenz (EFV; 24 hours) on mitochondrial parameters in primary cultures of rat cortical neurons and astrocytes. *A* and *B*, Determination of superoxide production, expressed as relative MitoSOX fluorescence (*A*), and mitochondrial membrane potential, shown as relative TMRM fluorescence (*B*), with increasing concentrations of EFV or vehicle (Veh), using rotenone (ROT) and FCCP (both at 10 μM), respectively, as positive controls. *C*, Effect of EFV on cell viability as measured by the MTT assay; results represent relative absorbance (λ = 570 nm) and are expressed as the percentage of the absorbance recorded in untreated cells. Data (mean ± standard error of the mean; n = 4–5) were compared to those of untreated cells (the values for which were considered 100%) and analyzed by the Student *t* test. $^{*}P < .05$, $^{**}P < .01$, and $^{***}P < .001$, compared with vehicle; $^{\#\#}P < .01$ and $^{\#\#\#}P < .001$ for comparisons of ROT and FCCP values to those for untreated cells.

produced in neurons and glial cells and provide the first evidence that neurons are more susceptible than glia to the negative effects of this drug on cell viability.

EFV Affects the Bioenergetics of Neurons and Glial Cells in Different Ways

Having confirmed that EFV compromises mitochondrial function, we next explored its effect on cellular bioenergetics. Inhibition of mitochondrial respiration is known to activate AMPK, a major sensor of cell energetic stress [14]. We observed that EFV (6 hours) induced a significant and concentration-dependent increase in AMPK phosphorylation in glia but not in neurons (Figure 3*A*). Longer incubation (24 hours) induced a significant and concentration-dependent increase in ATP levels in the former cells but not in the latter (Figure 3*B*). The lactate level in the extracellular medium, an indicator of glycolysis activation, was determined to clarify whether the augmented ATP concentration in glial cells was the result of enhanced glycolysis. We found a major, concentration-dependent increase in lactate generation in gli(a) (Figure 3*C*), an effect that was absent when a glucose-free or galactose-containing medium was used (Supplementary Figure 1), thus pointing to enhanced glycolysis. Once again, these effects were not observed in neurons. Coincubation (for 6 or 24 hours) of gli(a) with compound C, an inhibitor of AMPK, blocked the activation of glycolysis (Figure 3*D*). These findings were reproduced in primary cultures, where enhanced ATP (Figure 3*E*) and lactate (Figure 3*F*) levels were observed in astrocytes but not in neurons. Considered together, these results demonstrate that glycolysis is triggered as a result of the following sequence of events: mitochondrial inhibition, intracellular ATP reduction, and AMPK activation.

Effect of EFV Is Exacerbated in the Presence of a Proinflammatory Stimulus

To analyze whether a proinflammatory state in the brain exacerbates the effects of EFV on mitochondria, exogenous NO was added to the cell culture. As expected, DETA-NO undermined mitochondrial respiration in both neuronal and glial cell lines. This action was enhanced in the presence of EFV (10 μM; Figure 4*A*). EFV + DETA-NO also had an additive effect on the other 2 parameters of mitochondrial function assessed: superoxide production (Figure 4*B*) and $\Delta\psi_m$ (Figure 4*C*). DETA-NO alone produced an increase in mitochondrial superoxide in both SH-SY5Y and U-251MG. In accordance with previous reports [11], $\Delta\psi_m$ was diminished in neurons and increased in glia in the presence of DETA-NO alone, whereas EFV reduced this parameter in both cell populations, an effect that was more pronounced when DETA-NO was present. Regarding the activation of glycolysis, DETA-NO elicited an increase in intracellular ATP in the neuroblastoma, with no changes in the glioma cells; however, increased lactate generation was detected in both. Notably, the glycolytic effect of EFV exhibited only by the glioma cells was strengthened in the presence of exogenous NO, as displayed by the ATP level (Figure 4*D*) and lactate release (Figure 4*E*).

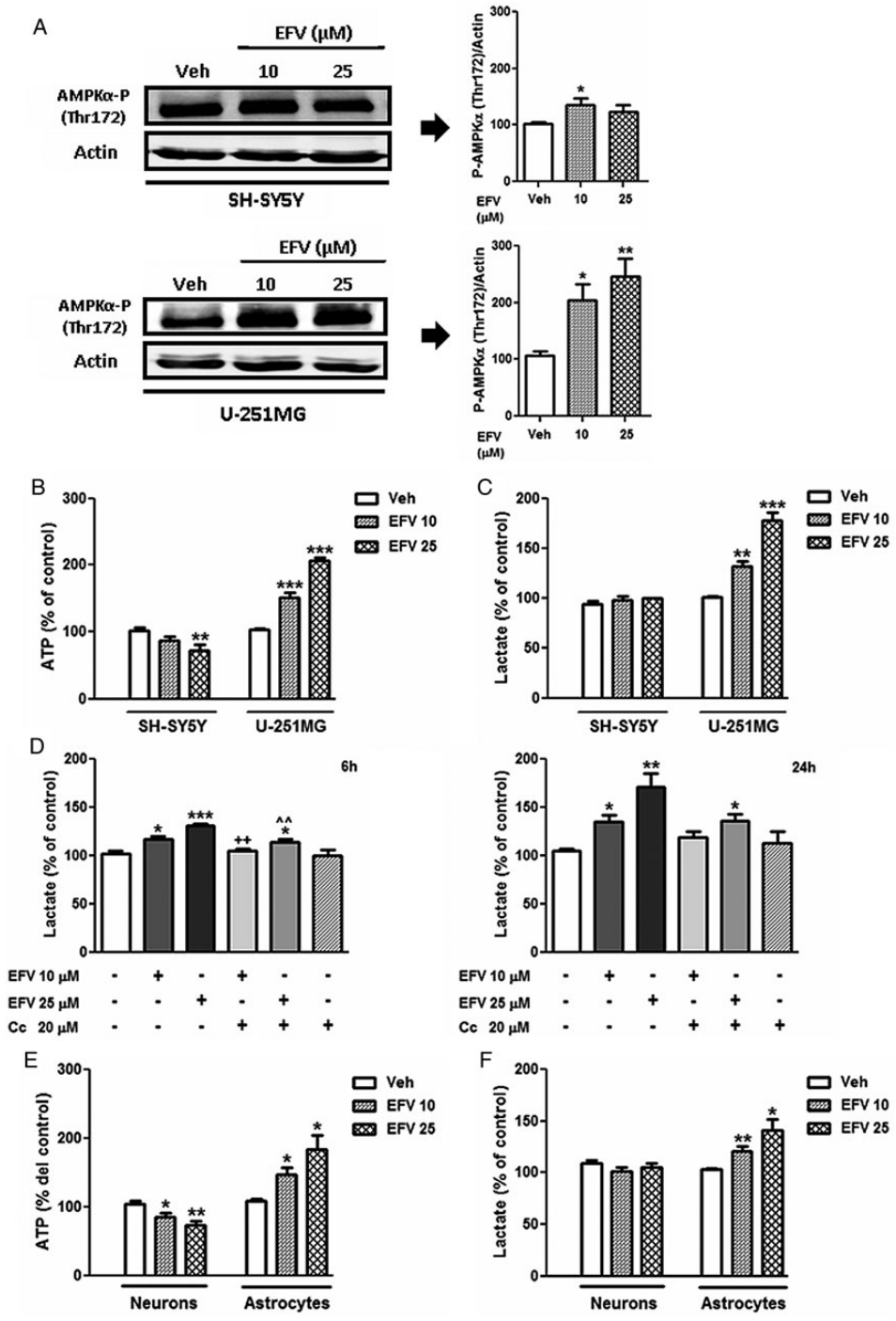

Figure 3. Efavirenz (EFV) produces a differential effect on cell bioenergetics in neurons and glia. *A*, SH-SY5Y (neuroblastoma cells) and U-251MG (glioma cells) were assessed for protein expression (Western blot) of phosphorylated AMPK (P-AMPK) in cells incubated without (vehicle; Veh) or with EFV for 6 hours. Representative images and histograms of the densitometric scans for the P-AMPK protein band, normalized with those of β-actin, are provided. Results show protein expression in relation to that of untreated cells in each individual experiment (considered 100%). *B*, Intracellular ATP levels were assessed in SH-SY5Y and U-251MG [illegible]urs after EFV treatment. *C*, Determination of the lactate level in the extracellular medium in cells treated with EFV for 24 hours. *D*, Determination of the lactate level in the extracellular medium of U-251MG cotreated with the AMPK inhibitor compound C (Cc) for 6 hours (left) and 24 hours (right). *E* and *F*, Primary cultures of neurons and astrocytes treated with vehicle or EFV for 24 hours were assessed for intracellular ATP levels (*E*) and lactate production ([illegible]in the extracellular medium. Data (mean ± standard error of the mean; n = 4–5 except for panel *D* [n = 3]) were compared to those for untreated cells (the values for which were considered 100%) and analyzed by the Student *t* test. $^{*}P < .05$, $^{**}P < .01$, $^{***}P < .001$, compared with vehicle; $^{++}P < .01$ for comparison of EFV10 to EFV10 + Cc; $^{\wedge\wedge}P < .01$ for comparison of EFV25 to EFV25 + Cc.

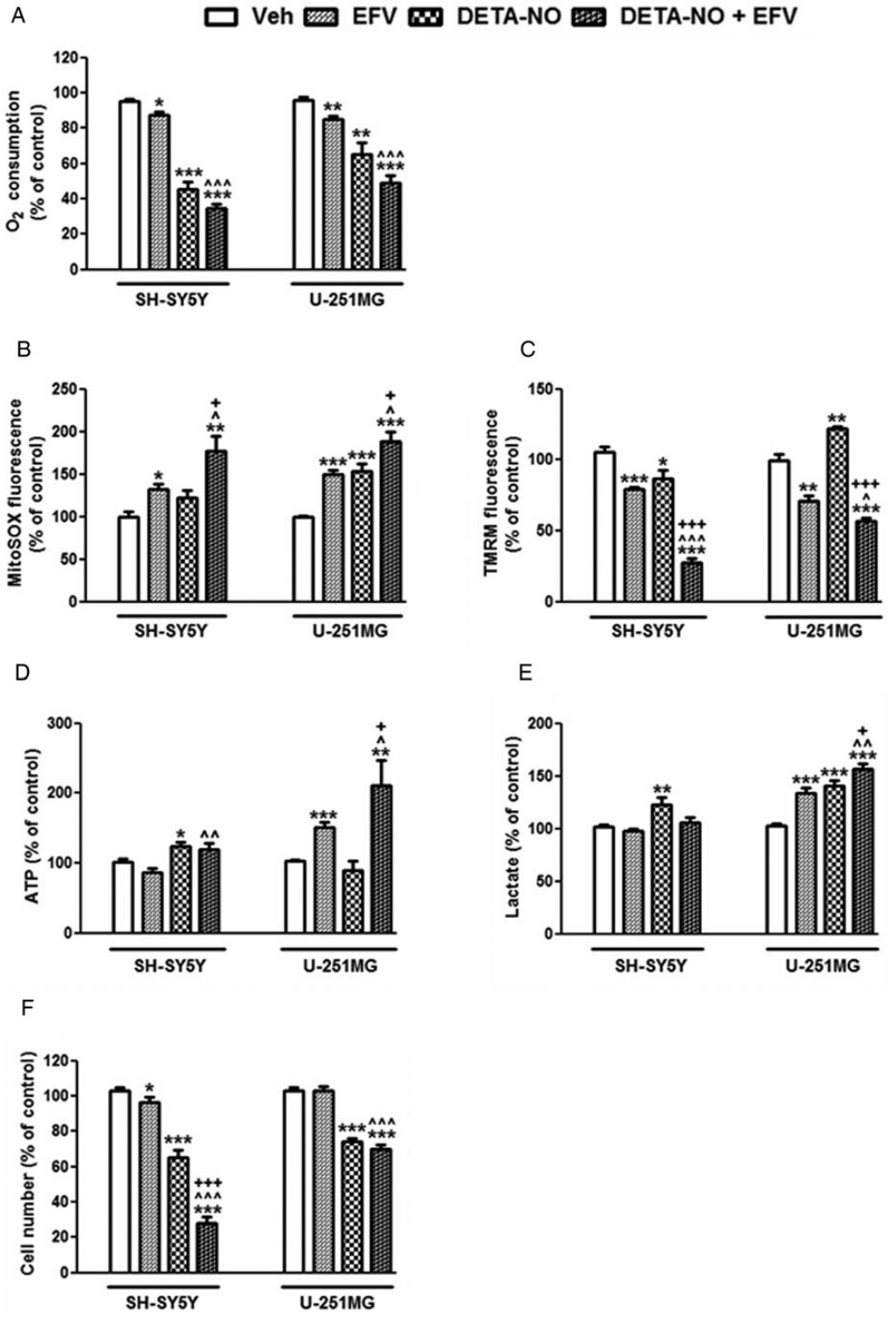

Figure 4. Effect of efavirenz (EFV) on SH-SY5Y (neuroblastoma cells) and U-251MG (glioma cells) in the presence of exogenous nitric oxide (NO). Histograms represent data obtained in the absence (vehicle; Veh) and presence of EFV 10 μM or DETA-NO (0.3 mM in neurons and 0.5 mM in glial cells) or cotreatment with DETA-NO + EFV 10 μM. *A*, O_2 consumption in intact cells of SH-SY5Y and U-251MG. *B–F*, At 24 hours, the effect of the combined treatment was evaluated according to the following parameters: mitochondrial redox state, in terms of superoxide production (*B*) and mitochondrial membrane potential (*C*); intracellular ATP level (*D*), lactate production (*E*), and cell number (*F*). Histograms represent cell count, determined by static cytometry (Hoechst fluorescence). Data (mean ± standard error of the mean; n = 3–5 were expressed as the percentage of the value for untreated cells (which was considered to be 100%) and analyzed by the Student *t* test. $^{*}P < .05$, $^{**}P < .01$, and $^{***}P < .001$, compared with vehicle; $^{\wedge}P < .05$, $^{\wedge\wedge}P < .01$, and $^{\wedge\wedge\wedge}P < .001$ for comparisons of EFV 10 μM to DETA-NO + EFV 10 μM); $^{+}P < .05$ and $^{+++}P < .001$ for comparisons of DETA-NO to cotreatment of DETA-NO + EFV 10 μM.

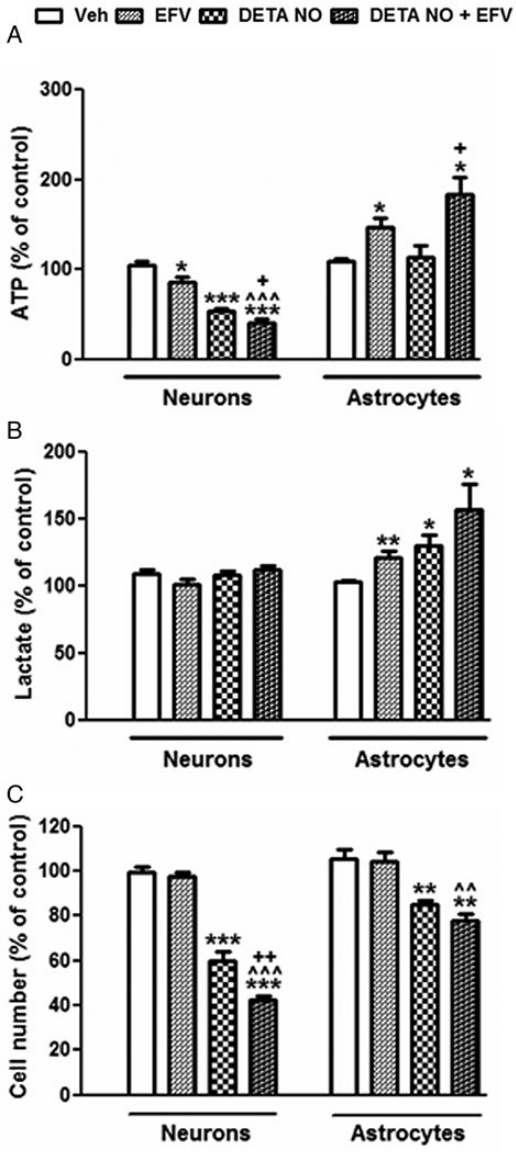

Figure 5. Effect of efavirenz (EFV) on primary cultures of neurons and astrocytes in the presence of exogenous nitric oxide (NO). Histograms represent data obtained in the absence (vehicle; Veh) and presence of EFV 10 μM, DETA-NO (0.3 mM in neurons and 0.5 mM in glial cells), or cotreatment with DETA-NO + EFV 10 μM for 24 hours. *A–C*, Intracellular adenosine triphosphate level (*A*), lactate production (*B*), and cell number (*C*). Histograms represent cell count, determined by static cytometry (Hoechst fluorescence). Data (mean ± standard error of the mean; n = 3–5, except for panel *B* [n = 8]) were expressed as the percentage of the value for untreated cells (which was considered to be 100%) and analyzed by the Student *t* test. **P* < .05, ***P* < .01, ****P* < .001, compared with vehicle; ^^*P* < .01 and ^^^*P* < .001 for comparisons of EFV 10 μM to DETA-NO + EFV 10 μM; ^{+}P < .05 and ^{++}P < .01 for comparisons of DETA-NO to DETA-NO + EFV 10 μM.

Finally, we aimed to evaluate whether this additive action of DETA-NO and EFV had consequences for the cell number and viability (Figure 4*F*). DETA-NO depleted the number of neuroblastoma and glioma cells, with the previous cells being more susceptible. EFV (10 μM) alone provoked only a slight reduction in the number of SH-SY5Y, an effect that was enhanced when these cells were cotreated with exogenous NO. Importantly, in U-251MG, the combined treatment did not aggravate the effect of DETA-NO. These findings are relevant for further understanding of the differential bioenergetic action elicited by EFV. Although mitochondrial parameters were additionally affected when EFV was used together with DETA-NO in both cell lines (with a significant additive effect in superoxide production and a decrease in $\Delta\psi_m$), glioma cells maintained their viability, whereas neuroblastoma cells significantly decreased in numbers/viability, compared with EFV or DETA-NO treatments alone. As bioenergetic characteristics are different in the 2 cell types, it seems that the synergistic effect of EFV + DETA-NO in triggering glycolysis in glioma cells enables them to maintain their viability, whereas the lack of enhanced glycolysis in the neuroblastoma cells makes them more vulnerable to the addition of a second mitotoxic stimulus.

In some of the experiments (ie, those assessing superoxide production and cell viability), cells were co-incubated with the NO scavenger PTIO (2-phenyl-4,4,5,5,-tetramethylimidazoline-1-oxyl 3-oxide) [15] to confirm that DETA-NO effects were due to the release of NO (data not shown). When primary cell cultures of glial cells and neurons were treated with EFV + DETA-NO (Figure 5), the additive effect on the bioenergetics was reproduced with slight variations. DETA-NO potentiated the enhancing effect of EFV on levels of ATP (Figure 5*A*) and lactate (Figure 5*B*) in astrocytes. However, DETA-NO produced a significant drop in ATP content in primary neurons that was potentiated in the presence of EFV, while no effect was exerted on lactate production. These differences between the responses of neuroblastoma cells and primary neurons were probably due to intrinsic metabolic differences. The experiment regarding cell number and viability in primary cell cultures reproduced the results obtained with the immortalized cell lines, showing an additive effect of EFV + DETA-NO in neurons but an absence of such an effect in astrocytes (Figure 5*C*).

DISCUSSION

The energetic requirements of the brain and the mechanisms by which it adapts to metabolic challenges are matters of debate, and particular controversy surrounds the role played by mitochondria. Substantial differences have been reported between the bioenergetics of glial cells (astrocytes, microglia, and oligodendrocytes) and neurons [1, 2]. Astrocytes, the only neural cell type with a reservoir of glycogen, are highly glycolytic [16, 17]. Neurons are not capable of maintaining ATP levels upon mitochondrial insult, which is crucial for cell viability, and they are therefore more vulnerable than g[illegible]0]. In the present work, we describe the effects of the antiretroviral drug EFV on the

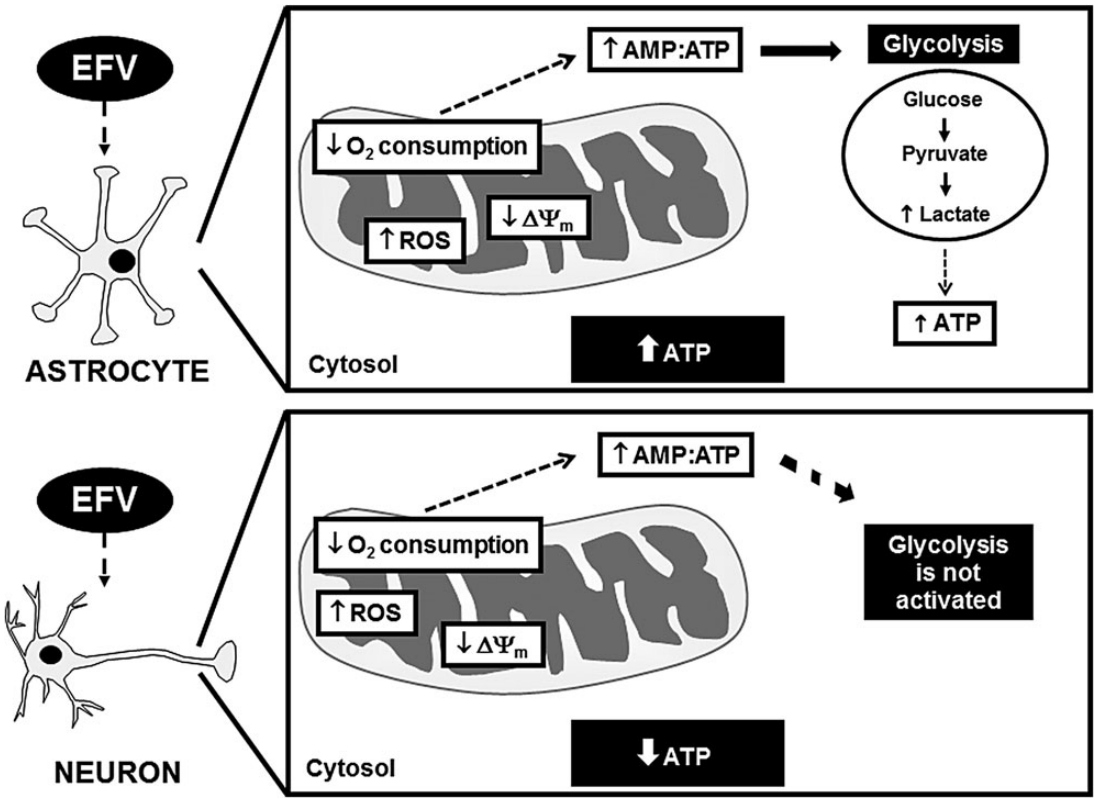

Figure 6. Schematic representation of the effect of efavirenz (EFV) on bioenergetics in glia and neurons. Abbreviation: AMP, adenosine monophosphate; ATP, adenosine triphosphate; ROS, reactive oxygen species; $\Delta\Psi_m$, mitochondrial membrane potential.

mitochondrial function, bioenergetics, and viability of glia and neurons. We observed that it altered mitochondrial respiration, enhanced reactive oxygen species generation, and undermined $\Delta\psi_m$ in a concentration-dependent fashion in both cell types. However, the implications of these effects for cell bioenergetics and survival varied in the 2 populations. In glia, EFV activated AMPK, leading to upregulated glycolysis and increased intracellular ATP levels, a response not observed in neurons. These results are in line with those of early reports hinting that inhibition of mitochondrial electron transport chain complexes with pharmacological reagents or energetic fluctuations affects glia and neurons in different ways [2, 18, 19]. More recently, a similar differential reaction to that observed in our experiments was described when complex IV (cytochrome *c* oxidase) of the mitochondrial electron transport chain was inhibited with NO [17]. As expected, NO produced mitochondrial hyperpolarization in glia in the present study, whereas EFV reduced $\Delta\psi_m$. To our knowledge, this is first evidence that glia and neurons respond differently to mitochondrial interference by clinical concentrations of a widely prescribed drug.

CNS toxicity is the main side effect of EFV use [4, 20–23] and is known to correlate with the drug plasma levels. The recommended daily dose of EFV for adults (600 mg) usually results in 3.17–12.67 μM in plasma [24], although much higher levels, even up to 73.6 μM, have been documented [20, 23, 25–27]. Although absolute cerebrospinal fluid levels of EFV differ from those in plasma, recent results show that protein-free levels are similar [28].

The cellular mechanisms responsible for the EFV-related CNS side effects are not understood, but there is evidence of deleterious actions of the drug on neuronal metabolism, as manifested by a reduced activity of creatine kinase, an enzyme involved in energy homeostasis, in different areas of the mouse brain [29]. Furthermore, 30 μM EFV undermined cell viability in primary cultures of rat astrocytes (24 hours), an effect related to mitochondria-generated oxidative stress [30]. In this context, it is relevant that EFV has recently been shown to affect mitochondrial complex IV in parts of the mouse brain [7] and to interfere with mitochondrial function in hepatocytes through acute and reversible inhibition of complex I, altering cellular bioenergetics and leading to mitophagy and cell death [8, 31].

HIV-infected individuals are prone to developing an inflammatory state in the brain, and up to 50% of these patients would eventually develop a neurological disorder [32]. Moreover, enhanced EFV-associated toxicity has been associated with increased inflammation in the CNS. For instance, the CNS-related EFV side effects are more likely to appear early after initiation of the treatment and usually coincide with the inflammatory state

that accompanies HIV infection per se in treatment-naive patients [5]. There is also evidence that EFV is associated with neurocognitive disorders in otherwise asymptomatic patients [6]. Finally, although the association is not flawless, there are also indications pointing to a higher frequency of EFV-induced CNS symptoms in conditions in which CNS neuroinflammation may play a role, such as some mental disorders [33] or chemical dependency [34].

NO is a major inflammatory mediator, and its upregulation underlies many neuropathological conditions [35]. Importantly, there is abundant evidence that HIV enhances brain NO synthesis [36, 37]. In addition, NO modulates mitochondrial respiration through a reversibly inhibiting complex IV and reacts with superoxide to form the highly deleterious reactive nitrogen species peroxynitrite. Of note, glial cells are more resistant than neurons to excess NO. Although this characteristic was initially thought to be a result of the robust antioxidant system of glial cells, it has been attributed more recently to the triggering of glycolysis and glucose uptake [17]. In our experiments, both DETA-NO and EFV altered mitochondrial function in glia and neurons, while they triggered AMPK activation and, in turn, glycolysis only in the former cell type. Of note, augmented ATP levels were not detected when glia were incubated with DETA-NO alone, probably because of the higher ATP consumption required for the maintenance and/or increase in $\Delta\psi_m$ [11]. Importantly, the effects of this NNRTI on human cancer cell lines were reproduced in primary cultures of rat cortical neurons and astrocytes, which rules out the possibility of them being specific to the cell model in question.

Because of its double action, both as a proinflammatory stimulator and a mitochondrial modulator, NO (in the form of DETA-NO) was used for EFV cotreatment analysis. EFV + DETA-NO coexposure resulted in a clear potentiation of their individual effects on mitochondrial parameters in both neurons and glia and enhanced ATP generation and lactate production in astrocytes. In terms of cell viability, EFV + DETA-NO cotreatment did not augment the depletion in the number of glial cells, but it did aggravate the damaging effect of NO on neurons. Excess NO could also mediate proinflammatory pathways in the brain by triggering apoptotic cell death or oxidative/nitrosative stress, both documented in HIV-positive patients [36, 38]. It is therefore relevant to remember that glial cells are an important reservoir of HIV, which may promote the existence of a confined inflammatory milieu in which neurons would be continuously under the action of NO. The relevance of this hypothesis, specifically in the context of EFV-induced side effects in the CNS, needs further evaluation, but, as already mentioned, a scenario of glial cell survival and neuron degeneration with signs of mitochondrial dysfunction and severe oxidative stress has been associated with HIV-associated neurocognitive disorders [3]. Again, our data are compatible with previous evidence that EFV exacerbates parameters associated with inflammation in the CNS [39] and carries a higher risk of HIV-associated neurocognitive disorders than other antiretrovirals [6].

In summary, EFV exercises a direct and specific effect on the energetic balance and viability of neurons and glia through a mechanism involving acute mitochondrial inhibition, and the effects are exacerbated under neuroinflammatory conditions, such as those often present in HIV-positive patients. The cell-specific mechanisms were obtained in vitro, and although they cannot be directly extrapolated to the human brain, we consider them to be of relevance in understanding the interaction between mitochondria-targeting compounds and CNS.

Supplementary Data

Supplementary materials are available at *The Journal of Infectious Diseases* online (http://jid.oxfordjournals.org/). Supplementary materials consist of data provided by the author that are published to benefit the reader. The posted materials are not copyedited. The contents of all supplementary data are the sole responsibility of the authors. Questions or messages regarding errors should be addressed to the author.

Notes

Acknowledgment. We thank Brian Normanly for his English language editing.

Financial support. This work was supported by the Instituto de Salud Carlos III, Ministerio de Economia y Competitividad (grants PI11/00327 and CIBER CB06/04/0071); the Conselleria d'Educació, Formació i Ocupació, Generalitat Valenciana (grants PROMETEO/2010/060 and ACOMP/2013/236); the Universitat de València (grant UV-INV-PRECOMP12-80613); the Conselleria d'Educació, Cultura i Esport, Generalitat Valenciana (grant BEST/2013/158 to N. [illegible]); the Generalitat Valenciana (predoctoral trainee research grant GRISOLIA/2010/40 to H. A. F.); and the Instituto de Salud Carlos III, Ministerio de Economía y Competitividad (predoctoral trainee research grant FI12/00198 to F. A.).

Potential conflicts of interest. All authors: No reported conflicts.

All authors have submitted the ICMJE Form for Disclosure of Potential Conflicts of Interest. Conflicts that the editors consider relevant to the content of the manuscript have been disclosed.

References

1. Bolaños JP, Almeida A, Moncada S. Glycolysis: a bioenergetic or a survival pathway? Trends Biochem Sci **2010**; 35:145–9.
2. Almeida A, Moncada S, Bolaños JP. Nitric oxide switches on glycolysis through the AMP protein kinase and 6-phosphofructo-2-kinase pathway. Nat Cell Biol **2004**; 6:45–51.
3. Saha RN, Pahan K. Differential regulation of Mn-superoxide dismutase in neurons and astroglia by HIV-1 gp120: Implications for HIV-associated dementia. Free Radic Biol Med **2007**; 42:1866–78.
4. Fumaz CR, Munoz-Moreno JA, Molto J, et al. Long-term neuropsychiatric disorders on efavirenz-based approaches: quality of life, psychologic issues, and adherence. J Acquir Immune Defic Syndr **2005**; 38:560–5.
5. Cavalcante GI, Capistrano VL, Cavalcante FS, et al. Implications of efavirenz for neuropsychiatry: a review. Int J Neurosci **2010**; 120:739–45.
6. Ciccarelli N, Fabbiani M, Di Giambenedetto S, et al. Efavirenz associated with neurocognitive disorders in otherwise asymptomatic HIV-infected patients. Neurology **2011**; 76:1403–9.
7. Streck EL, Ferreira GK, Scaini G, et al. Non-nucleoside reverse transcriptase inhibitors efavirenz and nevirapine inhibit cytochrome C oxidase in mouse brain regions. Neurochem Res **2011**; 36:962–6.

8. Blas-García A, Apostolova N, Ballesteros D, et al. Inhibition of mitochondrial function by efavirenz increases lipid content in hepatic cells. Hepatology **2010**; 52:115–25.
9. Apostolova N, Blas-García A, Esplugues JV. Mitochondrial interference by anti-HIV drugs: mechanisms beyond Pol-γ inhibition. Trends Pharmacol Sci **2011**; 32:715–25.
10. Kaul M. HIV-1 associated dementia: update on pathological mechanisms and therapeutic approaches. Curr Opin Neurol **2009**; 22:315–20.
11. Almeida A, Almeida J, Bolaños JP, Moncada S. Different responses of astrocytes and neurons to nitric oxide: the role of glycolytically generated ATP in astrocyte protection. Proc Natl Acad Sci U S A **2001**; 98:15294–99.
12. Sánchez S, Jiménez C, Carrera AC, Diaz-Nido J, Avila J, Wandosell F. A cAMP activated pathway, including PKA and PI3K, regulates neuronal differentiation. Neurochem Int **2004**; 44:231–42.
13. Almeida A, Medina JM. A rapid method for the isolation of metabolically active mitochondria from rat neurons and astrocytes in primary culture. Brain Res Brain Res Protoc **1998**; 2:209–14.
14. Hardie DG. AMP-activated/SNF1 protein kinases: conserved guardians of cellular energy. Nat Rev Mol Cell Biol **2007**; 8:774–85.
15. Goldstein S, Russo A, Samuni A. Reactions of PTIO and carboxy-PTIO with *NO, *NO2, and O2-*. J Biol Chem **2003**; 278:50949–55.
16. Wiesinger H, Hamprecht B, Dringen R. Metabolic pathways for glucose in astrocytes. Glia **1997**; 21:22–34.
17. Bolaños JP, Almeida A. Modulation of astroglial energy metabolism by nitric oxide. Antioxid Redox Signal **2006**; 8:955–65.
18. Erecińska M, Deas J, Silver IA. The effect of pH on glycolysis and phosphofructokinase activity in cultured cells and synaptosomes. J Neurochem **1995**; 65:2765–72.
19. Moncada S, Erusalimsky JD. Does nitric oxide modulate mitochondrial energy generation and apoptosis? Nat Rev Mol Cell Biol **2002**; 3:214–20.
20. Marzolini C, Telenti A, Decosterd LA, Greub G, Biollaz J, Buclin T. Efavirenz plasma levels can predict treatment failure and central nervous system side effects in HIV-1-infected patients. AIDS **2001**; 15:71–5.
21. Gutiérrez-Valencia A, Viciana P, Palacios R, et al. Stepped-dose versus full-dose efavirenz for HIV infection and neuropsychiatric adverse events: a randomized trial. Ann Intern Med **2009**; 151:149–56.
22. Gutiérrez F, Navarro A, Padilla S, et al. Prediction of neuropsychiatric adverse events associated with long-term efavirenz therapy, using plasma drug level monitoring. Clin Infect Dis **2005**; 41:1648–53.
23. Gounden V, van Niekerk C, Snyman T, George JA. Presence of the CYP2B6 516G> T polymorphism, increased plasma Efavirenz concentrations and early neuropsychiatric side effects in South African HIV-infected patients. AIDS Res Ther **2010**; 7:32.
24. Staszewski S, Morales-Ramirez J, Tashima KT, et al. Efavirenz plus zidovudine and lamivudine, efavirenz plus indinavir, and indinavir plus zidovudine and lamivudine in the treatment of HIV-1 infection in adults. Study 006 Team. N Engl J Med **1999**; 341:1865–73.
25. Taylor S, Reynolds H, Sabin CA, et al. Penetration of efavirenz into the male genital tract: drug concentrations and antiviral activity in semen and blood of HIV-1-infected men. AIDS **2001**; 15:2051–3.
26. Burger D, van der Heiden I, la Porte C, et al. Interpatient variability in the pharmacokinetics of the HIV non-nucleoside reverse transcriptase inhibitor efavirenz: the effect of gender, race, and CYP2B6 polymorphism. Br J Clin Pharmacol **2006**; 61:148–54.
27. Carr DF, la Porte CJ, Pirmohamed M, Owen A, Cortes CP. Haplotype structure of CYP2B6 and association with plasma efavirenz concentrations in a Chilean HIV cohort. J Antimicrob Chemother **2010**; 65:1889–93.
28. Avery LB, Sacktor N, McArthur JC, Hendrix CW. Protein-free efavirenz concentrations in cerebrospinal fluid and blood plasma are equivalent: applying the law of mass action to predict protein-free drug concentration. Antimicrob Agents Chemother **2013**; 57:1409–14.
29. Streck EL, Scaini G, Rezin GT, Moreira J, Fochesato CM, Romao PR. Effects of the HIV treatment drugs nevirapine and efavirenz on brain creatine kinase activity. Metab Brain Dis **2008**; 23:485–92.
30. Brandmann M, Tulpule K, Schmidt MM, Dringen R. The antiretroviral protease inhibitors indinavir and nelfinavir stimulate Mrp1-mediated GSH export from cultured brain astrocytes. J Neurochem **2012**; 120:78–92.
31. Apostolova N, Gomez-Sucerquia LJ, Gortat A, Blas-Garcia A, Esplugues JV. Compromising mitochondrial function with the antiretroviral drug efavirenz induces cell survival-promoting autophagy. Hepatology **2011**; 54:1009–19.
32. McArthur JC, Steiner J, Sacktor N, Nath A. Human immunodeficiency virus-associated neuroneurocognitive disorders: Mind the gap. Ann Neurol **2010**; 67:699–714.
33. Peyriere H, Mauboussin JM, Rouanet I, Fabre J, Reynes J, Hillaire-Buys D. Management of sudden psychiatric disorders related to efavirenz. AIDS **2001**; 15:1323–4.
34. Lochet P, Peyrière H, Lotthé A, Mauboussin JM, Delmas B, Reynes J. Long-term assessment of neuropsychiatric adverse reactions associated with efavirenz. HIV Med **2003**; 4:62–6.
35. Esplugues JV. NO as a signalling molecule in the nervous system. Br J Pharmacol **2002**; 135:1079–95.
36. Li W, Malpica-Llanos TM, Gundry R, et al. Nitrosative stress with HIV dementia causes decreased L-prostaglandin D synthase activity. Neurology **2008**; 70:1753–62.
37. Walsh KA, Megyesi JF, Wilson JX, Crukley J, Laubach VE, Hammond RR. Antioxidant protection from HIV-1 gp120-induced neuroglial toxicity. J Neuroinflammation **2004**; 1:8.
38. Li W, Galey D, Mattson MP, Nath A. Molecular and cellular mechanisms of neuronal cell death in HIV dementia. Neurotox Res **2005**; 8:119–34.
39. Davidson DC, Schifitto G, Maggirwar SB. Valproic acid inhibits the release of soluble CD40L induced by non-nucleoside reverse transcriptase inhibitors in human immunodeficiency virus infected individuals. PLoS One **2013**; 8:e59950.